Wan, Xingbang; Shi, Junjie; Qiu, Yuchao; Chen, Min; Li, Jianzhong; Liu, Changsheng; Taskinen, Pekka; Jokilaakso, Ari

The effect of 15 wt%Al_2O_3 addition on the equilibrium phase relations of CaO–SiO_2–TiO_2 system at 1400 °C in air

Published in:
Ceramics International

DOI:
10.1016/j.ceramint.2021.05.205

Published: 01/09/2021

Document Version
Peer-reviewed accepted author manuscript, also known as Final accepted manuscript or Post-print

The effect of 15 wt.%Al_2O_3 addition on the equilibrium phase relations of CaO-SiO_2-TiO_2 system at 1400 °C in air

Xingbang Wan[1], Junjie Shi[2,3,*], Yuchao Qiu[2,3], Min Chen[1], Jianzhong Li[2,3], Changsheng Liu[4], Pekka Taskinen[1], Ari Jokilaakso[1]

Affiliations:

[1] Department of Chemical and Metallurgical Engineering, School of Chemical Engineering, Aalto University, PO Box 16100, FI-00076 Aalto, Finland.

[2] School of Metallurgy, Northeastern University, Shenyang 110819, P. R. China.

[3] Key Laboratory for Ecological Metallurgy of Multimetallic Mineral (Ministry of Education), Northeastern University, Shenyang 110819, Liaoning, P. R. China.

[4] School of Material Science and Engineering, Northeastern University, Shenyang, P. R. China.

Emails for authors:

Xingbang Wan: xingbang.wan@aalto.fi

*Corresponding author, Junjie Shi: junjieshi@126.com

Yuchao Qiu, qiuyc2004@126.com

Min Chen, min.chen@aalto.fi

Jianzhong Li, lijz@mail.neu.edu.cn

Changsheng Liu, csliu@mai.neu.edu.cn

Pekka Taskinen, pekka.taskinen@aalto.fi

Ari Jokilaakso, ari.jokilaakso@aalto.fi

ORCID:

Xingbang Wan, 0000-0001-8378-7600

Junjie Shi, 0000-0002-8673-0404

Min Chen, 0000-0003-0544-4359

Pekka Taskinen, 0000-0001-8332-6230

Ari Jokilaakso, 0000-0003-0582-7181

Abstract: The combined processing of industrial wastes of titania-bearing slags with coal fly ash is an important part of the circular economy. In the present work, the effect of Al_2O_3 on the 1400 °C liquidus isotherms of the perovskite, rutile and tridymite primary phase fields in the CaO-SiO_2-TiO_2-Al_2O_3 system has been determined by employing a high-temperature equilibration-quenching technique, followed by X-ray Photoelectron Spectroscopy and Scanning Electron Microscopy-Energy Dispersive X-ray Spectrometry. Titanium was confirmed to be stable as TiO_2 in the present equilibria. The equilibrium solid phases of perovskite $CaO{\cdot}TiO_2$, rutile TiO_2 and tridymite SiO_2 were confirmed to be coexisting with the liquid oxide phase. The comparison of the addition of 0 to 15 wt.% Al_2O_3 was beneficial for expanding the primary phase field of perovskite to lower TiO_2 concentrations. Comparisons of the experimental 1400 °C isotherm with the predictions using FactSage and MTDATA databases confirmed some differences to the present experimental data, thus demonstrating the direction for updating the present thermodynamic titania-bearing oxide databases.

Keywords: Urban mining, titania-bearing slag, Al_2O_3, phase diagram, perovskite, FactSage

Introduction

Urban mining[1] has become a hot research topic due to the potential economic benefits from the high growth rate of solid waste and its high content of critical metals, e.g., Li, Co, Ni, Ti, and Al [2,3]. The concept of urban waste has been extended from waste electrical and electronic equipment (WEEE), spent Li-ion batteries (LIBs), and magnet scrap, etc. to include industrial wastes,[4] e.g., red mud, coal fly ash (a high Al_2O_3 waste), and titania-bearing furnace slags. The titania-bearing slags are by-products of the reduction smelting of vanadium titano-magnetite ore, producing 10 wt.% - 28 wt.% TiO_2[5] from blast furnace smelting or 40 wt.% - 70 wt.% TiO_2[6] from electric furnace smelting. In order to efficiently recover Ti values in the slag, different hydrometallurgical processes, including sulfuric acid leaching[7], alkaline roasting-leaching[8] and various pyrometallurgical processes including microwave assistant roasting[9], supergravity separation[10], and selective crystallization – separation[11], have been proposed. In the pyrometallurgical processes, the key idea is to enhance the Ti element concentration in a titania-enriched phase by modifying the slag composition[12]. Recent studies[13, 14] have revealed that the addition of Al_2O_3 to titania-bearing slags has an effect on the precipitation of titania as perovskite ($CaTiO_3$), rutile (TiO_2), and anosovite (Al_2TiO_5-$FeTi_2O_5$-$MgTi_2O_5$-Ti_3O_5). Once the enhanced crystallization mechanism by addition of Al_2O_3 is explained thoroughly, it will provide the basis for the combined processing of urban wastes of titania-bearing slags with high Al_2O_3-containing waste, such as coal fly ash.

The key to understanding the influence of Al_2O_3 on the precipitation behavior of titania-enriched phases is to clarify the effect of additions of Al_2O_3 on the equilibrium phase relations and isotherms. According to the composition characteristics[15], titania-bearing slags can be described by the CaO-SiO_2-TiO_2-MgO-Al_2O_3 system. The core binary, ternary, as well as part of the quaternary systems, including CaO-TiO_2[16,17], SiO_2-TiO_2[18-21], Al_2O_3-TiO_2[22-27], CaO-SiO_2-TiO_2[28-30], CaO-MgO-TiO_2[31], and CaO-Al_2O_3-SiO_2-TiO_2[32], have been extensively investigated during the past decades, while the quaternary and quinary systems have received less attention. Zhao et al.[33,34] carried out a series of equilibrium experiments in reducing conditions at carbon saturation, and the results were projected on quasi-ternary phase diagrams with fixed mass fraction ratios of $w(MgO)/w(CaO)$=0.2-0.72 and $w(Al_2O_3)/w(SiO_2)$=0.4-0.6. The equilibrium phase relations indicated the composition

range for anosovite. Correspondingly, Wang et al.[35,36] designed compositions higher than 40 wt.% Al_2O_3 to explore the optimized composition range for anosovite primary phase in the systems of CaO-SiO_2-TiO_2-10wt.% Al_2O_3 and CaO-SiO_2-TiO_2-10wt.% Al_2O_3-5 wt.% MgO in air. Shi et al. [37-45] determined the extent of the primary field of the perovskite phase for CaO-SiO_2-TiO_2-Al_2O_3-MgO systems with lower than 30 wt.% TiO_2 at fixed (10 wt.% - 30 wt.%) Al_2O_3 and (0 wt.% - 15 wt.%) MgO. Moreover, commercial thermodynamic databases in MTDATA[46], FactSage[47], and HSC[48] have been built based on different models. Nowadays, most of the databases are well optimized for low-order systems[49,50]; however, significant inconsistences occur in high-order systems due to the lack of experimental data. In conclusion, both the experimentally studied and calculated phase diagrams are far from being sufficient for understanding the boundaries of the primary fields of titania-enriched phases, which severely restricts the development of combined recycling processes for urban wastes.

Therefore, a long-term research focus on equilibrium phase relations has been conducted over the past years; an addition of 10 wt.% Al_2O_3 to the CaO-SiO_2-TiO_2 system was studied in our previous work[51]. In this study, the equilibrium phase relations with a fixed addition of 15 wt.% Al_2O_3 for bulk composition were experimentally studied at 1400 °C in air. The computation predictions obtained by using FactSage and MTDATA database are compared to the experimental results. The aim of this study is to provide new data that can be used to update the thermodynamic database, and to provide important guidance for the development of combined recycling processes for titania-bearing slags and coal fly ash.

Experimental

High purity reagents were employed to avoid the influence of impurities, and oxide powders of CaO (99.99 wt.%), SiO_2 (99.99 wt.%), TiO_2 (99.8 wt.%), and Al_2O_3 (99.99 wt.%) from Alfa Aesar were carefully weighed in predetermined ratios into 0.15g samples. Then the weighed samples were carefully mixed and pressed into cylindrical buttons and stored in a desiccator before equilibration annealing. In the present research, the Al_2O_3 concentration was fixed to 15 wt.% to establish the effects on the CaO-SiO_2-TiO_2 system and its equilibrium phase relations.

The equilibrium experiments were conducted by a high-temperature gas-condensed equilibration–quenching technique[52] in a vertical furnace (Nabertherm RHTV 120-150/18) with a temperature accuracy of ± 2 °C, as illustrated in Figure 1. The pressed sample was wrapped in a platinum foil suspended by a platinum wire in the even temperature zone of the tube furnace, in flowing air. The temperature of the uniform hot zone was first increased to 50 °C above the experimental temperature and kept at that temperature for 0.5 h to accelerate the dissolution processes for equilibrium, after which it was decreased to 1400 °C for a long enough time to guarantee that equilibrium was reached. Previous studies[40-45, 53, 54] with different compositions and temperatures have confirmed that 24 h is sufficient for titania-bearing slags to reach equilibration; therefore, each sample was heated for 24 h at the equilibrium temperature.

After equilibrium was reached, the sample was quenched directly into the iced water placed below the vertical tube. The equilibrium phase assemblages were thus frozen from a high temperature to room temperature. The quenched sample was dried and mounted in epoxy resin, polished, and coated by carbon for EDS (Energy Dispersive X-ray Spectrometer; Thermo Fisher Scientific, Waltham, MA, USA) analysis.

The oxidation state of the titanium following the experiments was verified by XPS (X-ray Photoelectron Spectroscopy) measurements using a Kratos Axis Ultra system (Kratos Analytical Ltd, Manchester, UK), equipped with a monochromatic Al Kα X-ray source. The measurement was performed using an analysis area of 0.3 mm × 0.7 mm, with 80 keV pass energy and 1 eV energy step. Individual areas of C 1s, Si 2p, Ca 2p, Ti 2p, O 1s were recorded. An SEM (Scanning Electron Microscope; Tescan, Brno, Czech Republic) coupled with an UltraDry silicon drift EDS was used for characterizing the equilibrium micrographs and compositions. The standards (Astimex, Ontario Canada) utilized in the EDS analyses were rutile (Ti Kα), quartz (Si Kα), anhydrite (Ca Kα), olivine (for O, Kα), and metallic aluminum (for Al, Kα). The raw EDS data were processed with NSS microanalysis software [50]. For each phase, at least six points or areas were randomly selected to ensure high accuracy, as indicated by the standard deviation of the average value. The Proza (Phi-Rho-Z) matrix correction procedure was employed for raw data processing before normalizing the analysis results [55].

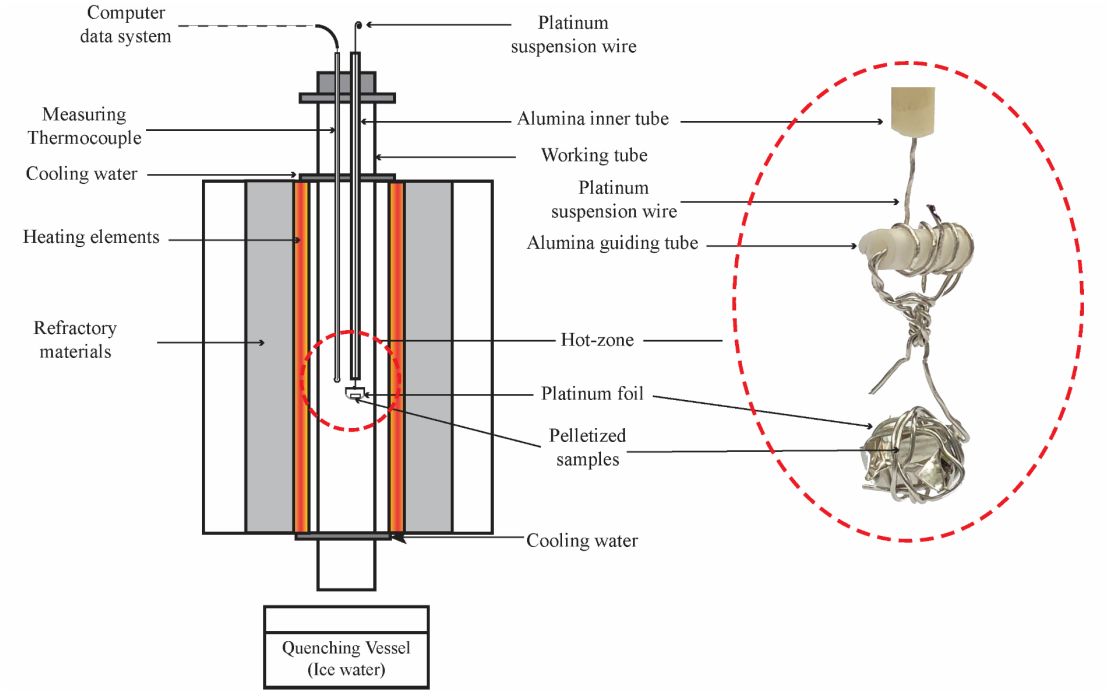

Figure 1. Graphical presentation of the vertical tube furnace used for the equilibrium experiments.

Results and Discussion

Determination of the oxidation state of Ti

It is essential to determine the oxidation state[56] when multi-valence elements are present in systems, such as titanium oxides in the quaternary CaO-SiO_2-TiO_2-Al_2O_3 system. As shown by the predominance phase diagram calculated by FactSage 8.0[57] (Figure 2(a)), titanium can be stable as TiO_2, Magneli phases, Ti_3O_5, Ti_2O_3, TiO, and Ti, depending on the temperature and oxygen partial pressure. As indicated by label A in Figure 2(a), titanium should be stable as TiO_2 under the present experimental conditions, i.e., at 1400 °C in air. An equilibrated sample was delivered for XPS analysis (Figure 2(b)) and the XPS spectra verified that titanium was present as Ti^{4+} in the equilibrium conditions. Thus, the titanium oxide was expressed as TiO_2 for all samples in the present quaternary sections.

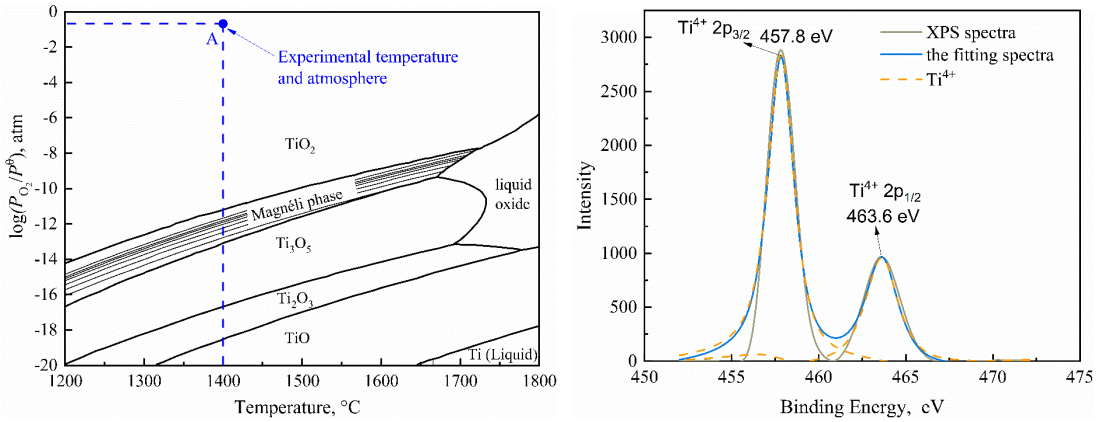

(a) Ti-O predominance area diagram (b) XPS result of Al15-14

Figure 2. Predominance phase diagram of the Ti-O system by FactSage (a) and the XPS spectrum for determining the oxidation state of titanium in the CaO-SiO_2-TiO_2-Al_2O_3 system in air of sample Al15-14 (b).

Equilibrium phase relations

The SEM micrographs as well as the compositions of the equilibrium phases with fixed 15 wt.% Al_2O_3 in the CaO-SiO_2-TiO_2 system are presented in Figure 3 and Table 1. In the composition range studied in the present work, one single liquid phase region, three two-phase co-equilibrium domains (liquid with tridymite, rutile, and perovskite, respectively), and one three-phase co-equilibrium region (liquid coexisting with rutile and tridymite) were found.

In Figure 3(a), an example of a liquid-tridymite primary phase field is shown by sample Al15-2, indicating that the initial composition of this sample is located inside the primary phase field of tridymite. Similarly, the initial composition of sample Al 15-11 is within the primary phase field of rutile, as proved by the equilibrium result in Figure 3(b). In contrast, in Figure 3(c), a three-phase co-equilibrium is shown for sample Al15-3 with liquid coexisting with tridymite and rutile. According to the primary phase fields' adjacent rule[58], the primary fields of tridymite and rutile are adjacent to each other. Furthermore, the liquid-perovskite primary field and single liquid are exhibited in Figure 3(d) and Figure 3(e) for samples Al15-23 and Al15-14, respectively.

Table 1. The compositions for the equilibrium phases at 1400 °C in air.

No.	Initial compositions, wt.%				Equilibrium phases	Equilibrium compositions, wt.%			
	TiO_2	SiO_2	CaO	Al_2O_3		TiO_2	SiO_2	CaO	Al_2O_3
Liquid									
Al15-12	5.00	40.00	40.00	15.00	Liquid	8.4 ± 0.1	39.9 ± 0.1	36.1 ± 0.1	15.7 ± 0.1
Al15-13	10.00	37.50	37.50	15.00	Liquid	8.5 ± 0.1	40.0 ± 0.4	35.8 ± 0.5	15.7 ± 0.2
Al15-15	20.00	32.50	32.50	15.00	Liquid	21.6 ± 0.1	32.8 ± 0.1	29.7 ± 0.1	16.0 ± 0.0(4)
Al15-16	25.00	30.00	30.00	15.00	Liquid	26.8 ± 0.1	30.7 ± 0.1	27.3 ± 0.1	15.2 ± 0.0(4)
Al15-17	30.00	27.50	27.50	15.00	Liquid	35.9 ± 0.3	25.5 ± 0.3	23.8 ± 0.1	14.9 ± 0.1
Al15-18	35.00	25.00	25.00	15.00	Liquid	32.6 ± 0.1	21.8 ± 0.1	20.4 ± 0.1	25.2 ± 0.2
Al15-19	40.00	22.50	22.50	15.00	Liquid	36.2 ± 0.1	25.3 ± 0.1	23.7 ± 0.1	14.8 ± 0.1
Liquid+ Tridymite									
Al15-1	5.00	66.67	13.33	15.00	liquid	6.4 ± 0.7	65.0 ± 1.9	12.5 ± 1.4	16.1 ± 2.3
					Tridymite	0.9 ± 0.1	97.1 ± 3.9	0.7 ± 0.2	1.4 ± 0.1
Al15-2	10.00	62.50	12.50	15.00	Liquid	11.5± 1.8	63.1 ± 2.9	11.1 ± 1.4	14.4 ± 0.9
					Tridymite	0.6 ± 0.1	99.3 ± 1.5	0.0	0.1 ± 0.0(3)
Liquid+Perovskite									
Al15-14	15.00	35.00	35.00	15.00	Liquid	9.0 ± 0.1	30.9 ± 0.1	39.9 ± 0.0(4)	20.3 ± 0.0(3)
					Perovskite	58.8 ± 0.1	0.2 ± 0. 0(3)	40.8 ± 0.1	0.2 ± 0.0(3)
Al15-20	15.00	28.00	42.00	15.00	Liquid	12.1 ± 0.1	34.6 ± 0.1	36.6 ± 0.1	16.8 ± 0.2
					Perovskite	58.1 ± 0.5	0.2 ± 0.1	40.9 ± 0.1	0.7 ± 0.2
Al15-21	20.00	26.00	39.00	15.00	Liquid	16.0 ± 0.1	32.7 ± 0.2	32.3 ± 0.2	19.1 ± 0.4
					Perovskite	58.3 ± 0.3	0.1 ± 0.0(4)	40.9 ± 0.1	0.7 ± 0.2
Al15-22	25.00	24.00	36.00	15.00	Liquid	23.5 ± 0.1	28.8 ± 0.4	28.9 ± 0.2	18.8 ± 0.5
					Perovskite	58.6 ± 0.3	0.1 ± 0.0(4)	40.8 ± 0.1	0.5 ± 0.2
Al15-23	30.00	22.00	33.00	15.00	Liquid	29.6 ± 0.5	25.8 ± 0.5	26.7 ± 0.5	17.8 ± 0.4
					Perovskite	58.6 ± 0.1	0.1 ± 0.0(2)	40.9 ± 0.1	0.5 ± 0.0(4)
Al15-24	35.00	20.00	30.00	15.00	Liquid	37.5 ± 0.1	21.3 ± 0.1	25.3 ± 0.1	15.9 ± 0.1
					Perovskite	58.4 ± 0.5	0.0	41.0 ± 0.7	0.5 ± 0.1
Liquid+ Rutile									
Al15-4	20.00	54.17	10.83	15.00	Liquid	14.2 ± 0.8	57.8 ± 1.0	10.5 ± 0.4	17.5 ± 0.3
					Rutile	98.5 ± 0.2	0.3 ± 0.1	0.4 ± 0.1	0.8 ± 0.0(4)
Al15-5	25.00	50.00	10.00	15.00	Liquid	14.6 ± 0.4	55.6 ± 1.7	10.8 ± 0.4	19.0 ± 1.0
					Rutile	98.5 ± 0.1	0.3 ± 0.0(4)	0.3 ± 0.1	0.9 ± 0.1

Al15-7	35.00	41.67	8.33	15.00	Liquid	13.7 ± 0.1	57.5 ± 0.1	9.3 ± 0.0(3)	19.5 ± 0.1
					Rutile	98.1 ± 0.2	0.5 ± 0.1	0.2 ± 0.0(1)	1.1 ± 0.2
Al15-9	30.00	39.29	15.71	15.00	Liquid	21.4 ± 0.3	46.1 ± 0.8	15.5 ± 0.2	17.0 ± 0.5
					Rutile	98.8 ± 0.1	0.2 ± 0.0(3)	0.3 ± 0.1	0.7 ± 0.0(4)
Al15-10	35.00	35.71	14.29	15.00	Liquid	22.6 ± 0.2	43.6 ± 0.1	15.9 ± 0.1	17.8 ± 0.2
					Rutile	98.9 ± 0.1	0.2 ± 0.0(3)	0.2 ± 0.1	0.7 ± 0.0(4)
Al15-11	40.00	32.14	12.86	15.00	Liquid	22.7 ± 0.3	42.7 ± 0.3	14.5 ± 0.1	20.1 ± 0.2
					Rutile	98.6 ± 0.3	0.3 ± 0.1	0.2 ± 0.1	0.9 ± 0.0(4)
Liquid+Tridymite+Rutile									
Al15-3	15.00	58.33	11.67	15.00	Liquid	15.9 ± 1.5	59.0 ± 2.9	11.2 ± 1.1	13.9 ± 0.4
					Rutile	98.8 ± 0.1	0.2 ± 0.0(2)	0.4 ± 0.1	0.6 ± 0.0(2)
					Tridymite	0.9 ± 0.1	98.4 ± 1.3	0.0	0.6 ± 0.0(4)
Al15-6	30.00	45.83	9.17	15.00	Liquid	14.5 ± 1.2	55.3 ± 2.9	10.0 ± 1.5	20.2 ± 1.5
					Rutile	98.5 ± 0.2	0.3 ± 0.0(4)	0.2 ± 0.0(2)	1.1 ± 0.2
					Tridymite	3.0 ± 0.2	95.9 ± 0.7	0.0	1.1 ± 0.3
Al15-8	40.00	37.50	7.50	15.00	Liquid	14.3 ± 0.2	53.4 ± 0.5	9.4 ± 0.0(2)	22.9 ± 0.6
					Rutile	98.3 ± 0.3	0.2 ± 0.0(4)	0.2 ± 0.0(2)	1.2 ± 0.2
					Tridymite	0.2 ± 0.0(3)	99.8 ± 0.0(1)	0.0	0.0

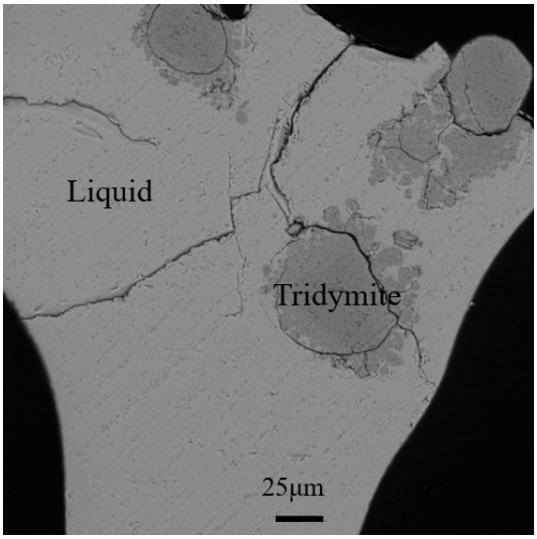

(a) Al15-2

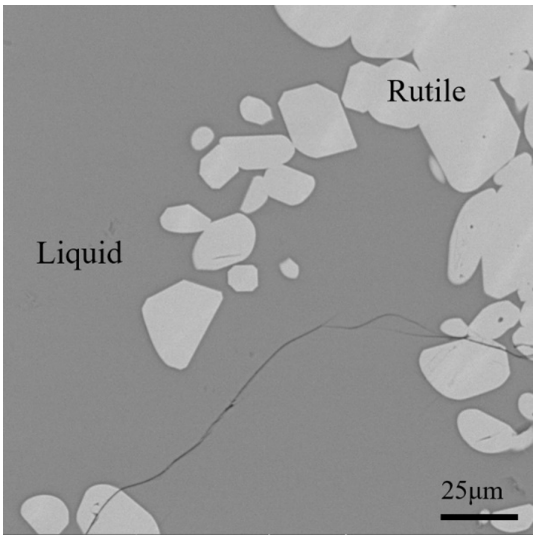

(b) Al15-11

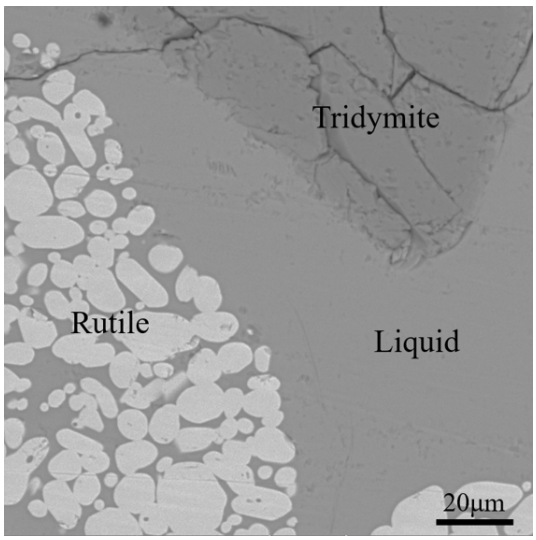

(c) Al15-3

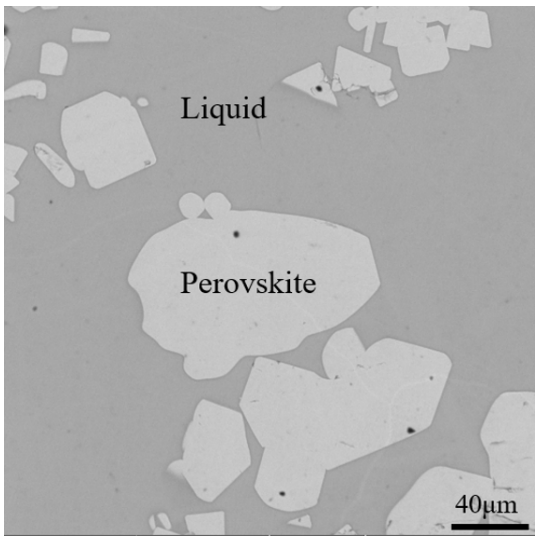

(d) Al15-23

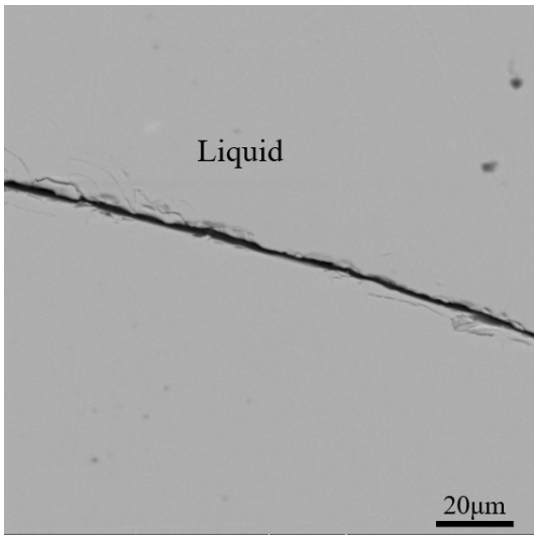

(e) Al15-14

Figure 3. Micrographs for the equilibrium phase domains at 1400 °C in air for the CaO-SiO_2-TiO_2-15 wt.% Al_2O_3 system.

Projections of the 1400 °C isotherm

Based on the experimental results discussed above, the 1400 °C isotherm with the fixed addition of 15 wt.% Al_2O_3 was projected and plotted in the quasi-ternary CaO-SiO_2-TiO_2 triangle with solid lines, as shown in Figure 4. The normalization used for estimating the equilibrium compositions exactly on the 15 wt.% Al_2O_3 plane in the quaternary system of CaO-SiO_2-TiO_2-Al_2O_3 has been reported in detail in our previous publications [38-45].

The equilibrium liquid compositions were projected together with the liquidus isotherms and are shown in Figure 4. The computational prediction by FactSage 8.0 for the locations of the primary phase fields were also plotted, along with the experimental results. The calculation was done by employing the "FactPS" and "FToxid" databases [59] in the phase diagram module with the oxygen partial pressure P_{O_2} set to 0.21 atm. As can be seen in Figure 4, the predicted 1400 °C isotherm for the tridymite and rutile primary phase fields agrees well with the present experimental results. However, the calculated 1400 °C isotherm for the liquid-perovskite primary phase field shifts significantly to higher SiO_2 concentrations. This deviation may come from the description by the software itself that the oxide database related to TiO_x was mainly optimized in a reducing atmosphere for low-order systems.

The 1400 °C isotherm predicted by MTDATA 7.1 [46] was projected in Figure 5 for a comprehensive comparison with the present results and the calculations from FactSage. The MTDATA calculations were carried out by employing the Mtox 8.2 and Mtoxsup databases, where a full assessment of the CaO-Fe-Ti-O-MgO-Al_2O_3-SiO_2 system is available [60]. This means that, e.g., anorthite and plagioclase are terminal phases of a large solid solution phase called 'feldspar'. Rutile, pseudobrookite, and perovskite are also solid solutions, whereas sphene ($CaSiTiO_5$) is a stoichiometric compound. In Figure 5, the 1400 °C isotherm predicted by MTDATA is labeled with dash-dot-dash lines. The major difference between FactSage and MTDATA is that sphene is not predicted to form as a primary phase by the Mtox database. Furthermore, the 1400 °C isotherm predicted by MTDATA is much more consistent with the present experimental results compared with the FactSage calculations. The experimental results of the present work are therefore important for the updating of present thermodynamic titania-bearing oxide databases.

The experimental results by DeVries et al. [61] and Chen et al. [51] were projected on Figure 6 to reveal the influence of 0 wt.% Al_2O_3, 10 wt.% Al_2O_3, and 15 wt.% Al_2O_3 on the 1400 °C liquidus isotherms in air. It can be concluded from Figure 6 that the addition of Al_2O_3 has an clear impact on the positions of the two-phase equilibrium isotherms. The addition of 10 wt.% and 15 wt.% Al_2O_3 was beneficial for extending the liquid-perovskite equilibrium to lower TiO_2 concentrations. This is useful for industrial applications for the modification of titania-bearing slag with an expanding composition range by a selective crystallization and separation technique. Similarly, the addition of 10 wt.% and 15 wt.% Al_2O_3 leads to the location of the liquid-rutile equilibrium isotherm moving to a lower TiO_2 and lower $w(CaO)/w(SiO_2)$ ratio region, which results in the significant shrinkage of the liquid-tridymite equilibrium area.

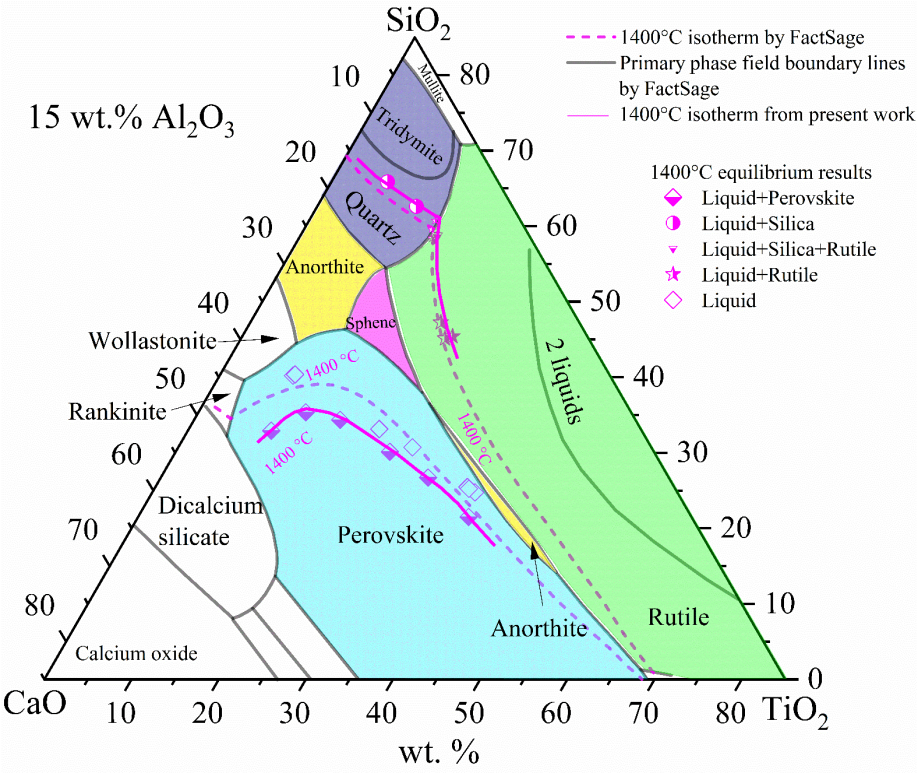

Figure 4. The 1400 °C liquidus isotherms for the CaO-SiO_2-TiO_2 system containing 15 wt.% Al_2O_3. The primary phase fields are described according to FactSage simulations.

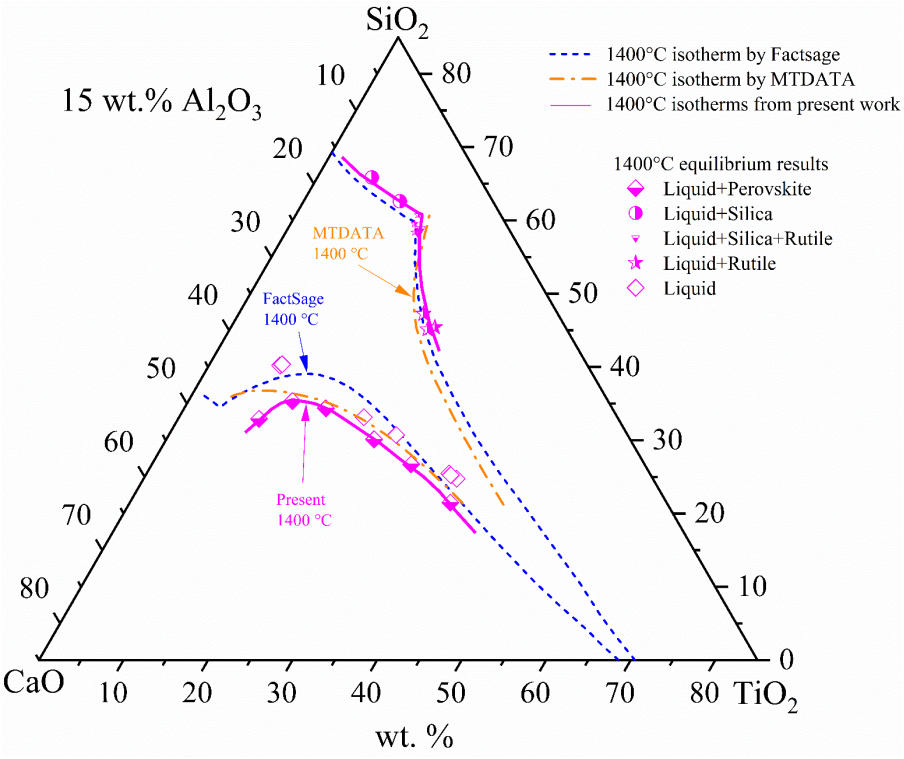

Figure 5. Comparison of the 1400 °C liquidus isotherms with the predictions by FactSage and MTDATA.

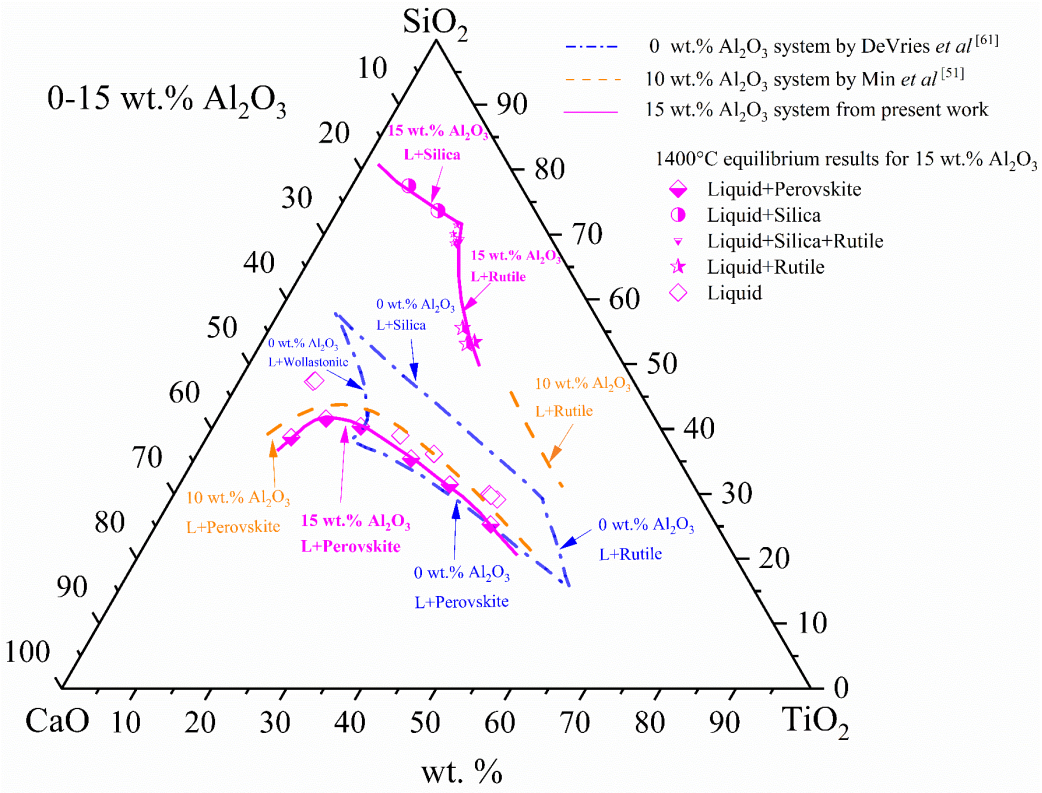

Figure 6. Projections of the 1400 °C liquidus isotherms for selected CaO-SiO_2-TiO_2-Al_2O_3 slag compositions on to the CaO-SiO_2-TiO_2 system.

Conclusions

In order to realize the combined recycling of titania-bearing slags and high Al_2O_3-containing wastes such as coal fly ash, the thermodynamic mechanism of the addition of Al_2O_3 in the equilibrium phase evolution was experimentally determined by a high-temperature thermodynamic equilibration-quenching technique. The results were compared with computational predictions by FactSage and MTDATA, as well as with results in the previous literature.

The XPS analysis confirmed that Ti was stable as TiO_2 under the present experimental conditions, confirming that the equilibrium phases containing Ti element can be expressed by the highest valence as Ti^{4+}. The 1400 °C isotherm from the present work was projected onto the quasi-ternary phase diagram of CaO-SiO_2-TiO_2. The differences, confirmed by the comparisons with FactSage and MTDATA calculations, indicate the direction for updating the present thermodynamic titania-bearing oxide databases. This is important for providing accurate data and establishing the related process parameters.

Acknowledgements

The authors wish to acknowledge the contributions of Aalto University. This study utilized the Academy of Finland's RawMatTERS Finland Infrastructure (RAMI) housed jointly at Aalto University, GTK, and VTT in Espoo.

Disclosure statement

The authors report no conflicts of interest and the authors alone are responsible for the content and writing of the article.

Funding
This study received financial support from Aalto University. The authors would also like to acknowledge the financial support from the China Postdoctoral Science Foundation [Grant number 2020TQ0059, 2020M680967], the Fundamental Research Funds for the Central Universities [N2125010] and China Scholarship Council [Grant number 201706370096, 201806370217].

Reference

[1] R. Cossu and I.D. Williams, Urban mining: Concepts, terminology, challenges, *Waste Manage*. 45 (2015) 1-3. https://doi.org/10.1016/j.wasman.2015.09.040.

[2] J. Shi, C. Peng, M. Chen, Y. Li, H. Eric, L. Klemettinen, M. Lundström, P. Taskinen, A. Jokilaakso, Sulfation Roasting Mechanism for Spent Lithium-Ion Battery Metal Oxides Under SO_2 -O_2 -Ar Atmosphere, *JOM*, 71 (2019) 4473-4482.
https://doi.org/10.1007/s11837-019-03800-5.

[3] X. Wan, P. Taskinen, J. Shi, and A. Jokilaakso. A potential industrial waste–waste co-treatment process of utilizing waste SO_2 gas and residue heat to recover Co, Ni, and Cu from copper smelting slag, *J. Hazard. Mater.*, (2021): 125541.
https://doi.org/10.1016/j.jhazmat.2021.125541.

[4] Z. Sun, Y. Xiao, H. Agterhuis, J. Sietsma, Y. Yang, Recycling of metals from urban mines-a strategic evaluation, *J. Clean Prod*. 112 (2016) 2977-2987.
https://doi.org/10.1016/j.jclepro.2015.10.116.

[5] J. Li, Z. Zhang, M. Zhang, M. Guo, X. Wang, The influence of SiO_2 on the extraction of Ti element from Ti-bearing blast furnace slag, *Steel Res. Int.* 82 (2011) 607-614.
https://doi.org/10.1002/srin.201000217.

[6] S. Ren, J. Zhang, L. Wu, W. Liu, Y. Bai, X. Xing, B. Su, D. Kong, Influence of B_2O_3 on viscosity of high Ti-bearing blast furnace slag, *ISIJ Int.* 52 (2012) 984-991.
https://doi.org/10.2355/isijinternational.52.984.

[7] S. He, H. Sun, D. Tan, T. Peng, Recovery of titanium compounds from Ti-enriched product of alkali melting Ti-bearing blast furnace slag by dilute sulfuric acid leaching, *Procedia Environ. Sci.* 31 (2016) 977-984. https://doi.org/10.1016/j.proenv.2016.03.003.

[8] D. S. Chen，L. S. Zhao，T. Qi，G. P. Hu，H. X. Zhao，J. Li，L. N. Wang, Desilication from titanium–vanadium slag by alkaline leaching, *Trans. Nonferrous Met. Soc. China* 23 (2013) 3076-3082. https://doi.org/10.1016/S1003-6326(13)62836-8.

[9] Z. Han, J. Gao, X. Yuan, Y. Zhong, X. Ma, Z. Chen, D. Luo, Y. Wang, Microwave roasting of blast furnace slag for carbon dioxide mineralization and energy analysis, *RSC Adv*. 10 (2020) 17836-17844. DOI: 10.1039/D0RA02846K.

[10] Y. Lu, J. Gao, F. Wang, Z. Guo, Separation of anosovite from modified titanium-bearing slag melt in a reducing atmosphere by supergravity, *Metall. Mater. Trans. B* 48 (2017) 749-753. DOI: 10.1007/s11663-016-0868-6.

[11] X. Wan, M. Chen, Y. Qiu, J. Shi, J. Li, C. Liu, P. Taskinen, A. Jokilaakso, Influence of manganese oxide on the liquid-perovskite equilibrium in the CaO-SiO_2-TiO_2 system at 1400 °C in air*, Ceram. Int* 47, no. 8 (2021) 11176-11182. https://doi.org/10.1016/j.ceramint.2020.12.241. https://doi.org/10.1016/j.ceramint.2020.12.241

[12] J. Li, X. Wang, Z. Zhang, Crystallization behavior of rutile in the synthesized Ti-bearing blast furnace slag using single hot thermocouple technique, *ISIJ Int.* 51 (2011) 1396-1402. https://doi.org/10.2355/isijinternational.51.1396.

[13] L. Sun, J. Shi, Effect of Al_2O_3 Addition on the Phase Equilibria Relations of CaO-SiO_2-5 wt% MgO-Al_2O_3-TiO_2 System Relevant to Ti-bearing Blast Furnace Slag*, ISIJ Int.* 59 (2019) 1184-1191. https://doi.org/10.2355/isijinternational.ISIJINT-2019-014.

[14] Z. Li, J. Li, Y. Sun, S. Seetharaman, L. Liu, X. Wang, Z. Zhang, Effect of Al_2O_3 addition on the precipitated phase transformation in Ti-bearing blast furnace slags, *Metall. Mater. Trans. B* 47 (2016) 1390-1399. DOI: 10.1007/s11663-015-0576-7.

[15] J. Liao, J. Li, X. Wang, Z. Zhang, Influence of TiO_2 and basicity on viscosity of Ti bearing slag, *Ironmak. Steelmak*. 39 (2012) 133-139. https://doi.org/10.1179/1743281211Y.0000000064.

[16] A. Jongejan, A. Wilkins, A re-examination of the system CaO-TiO_2 at liquidus temperatures, *J Less Common Met*. 20 (1970) 273-279. https://doi.org/10.1016/0022-5088(70)90001-9.

[17] W. Gong, L.Wu and A.Navrotsky, Combined experimental and computational investigation of thermodynamics and phase equilibria in the CaO-TiO_2 system. *J. Am. Ceram. Soc.*, 101(3), (2018) 1361-1370. https://doi.org/10.1111/jace.15286.

[18] S. Kirillova, V. Almjashev, V. Gusarov, Phase relationships in the SiO_2-TiO_2 system, *Russ. J. Inorg. Chem*. 56 (2011) 1464.https://doi.org/10.1134/S0036023611090117.

[19] R. DeVries, R.Roy and E.Osborn, The system TiO_2-SiO_2. *Trans. J. Br. Ceram. Soc.*, 53, (1954) 525-540. https://doi.org/10.1111/j.1151-2916.1955.tb14922.x.

[20] E. Bunting, Phase equilibria in the systems TiO_2, TiO_2-SiO_2, and TiO_2-Al_2O_3. *Bur. Stand. J. Res.*, 11(5), (1933)719-25.

[21] R. Ricker and F. Hummel, Reactions in the system TiO_2-SiO_2; revision of the phase diagram. *J. Am. Ceram. Soc.*, 34(9), (1951)271-279.

[22] S.T. Norberg, S. Hoffmann, M. Yoshimura, N. Ishizawa, $Al_6Ti_2O_{13}$, a new phase in the Al_2O_3–TiO_2 system, *Acta Crystallogr. Sect. C-Cryst. Struct. Commun*. 61 (2005) i35-i38. https://doi.org/10.1107/S0108270105002532.

[23] S. Lang, C. Fillmore and L. Maxwell, The system beryllia-alumina-titania: phase relations and general physical properties of three-component porcelains. *J. Res. Natl. Bur. Stand.*, 48, (1952) 298-312.

[24] I. Jung, G. Eriksson, P. Wu and A. Pelton, Thermodynamic modeling of the Al_2O_3-Ti_2O_3-TiO_2 system and its applications to the Fe-Al-Ti-O inclusion diagram. *ISIJ Int.*, 49(9), (2009) 1290-1297. https://doi.org/10.2355/isijinternational.49.1290

[25] M. Ilatovskaia, G. Savinykh, and O. Fabrichnaya, Thermodynamic description of the Ti-Al-O system based on experimental data. *J. Phase Equilib. Diffus.*, 38(3), (2017)175-184. https://doi.org/10.1007/s11669-016-0509-4

[26] K. Das, P. Choudhury and S. Das, The Al-O-Ti (aluminum-oxygen-titanium) system. *J. Phase Equilib.*, 23(6), (2002) 525. https://doi.org/10.1361/105497102770331271

[27] M. Berger and A. Sayir, Directional solidification of Al_2O_3-Al_2TiO_5 system. *J. Eur. Ceram. Soc.*, 28(12), (2008)2411-2419. https://doi.org/10.1016/j.jeurceramsoc.2008.03.005

[28] H. Nakada, K. Nagata, Crystallization of CaO-SiO_2-TiO_2 slag as a candidate for fluorine free mold flux, *ISIJ Int.* 46 (2006) 441-449. https://doi.org/10.2355/isijinternational.46.441.

[29] G. Ye and T. Rosenqvist, Phase relations in the Ti-Si-Ca-O system under reducing conditions, and silicothermic reduction of titanium oxide. *Scand. J. Metall.*, 20(4), (1991) 222-228.

[30] V. Daněk and I. Nerád, Phase Diagram and Structure of Melts of the System CaO-TiO_2-SiO_2. *Chem. Pap*, 56(4), (2002)241-246.

[31] M. Rouf, A. Cooper, H. Bell, A study of phase equilibria in the system CaO-MgO-TiO_2, *Trans. J. Br. Ceram. Soc*. (1969) 263-267.

[32] A. Provodova, N. Yakushevich, N. Kozyrev, Thermodynamic activity of the liquid-phase components in the $CaO{\cdot}SiO_2$-$CaO{\cdot}Al_2O_3{\cdot}2SiO_2$-$CaO{\cdot}TiO_2{\cdot}SiO_2$ system with four-phase invariant equilibrium, *Steel Transl.* 43 (2013) 474-479. https://doi.org/10.3103/S096709121308010X.

[33] B. Zhao, E. Jak, P.C. Hayes, Phase equilibria studies in the slag system "TiO_2-CaO-MgO-Al_2O_3-SiO_2" at carbon saturation, in: VIII International Conference on Molten Slags, Fluxes and Salts, Santiago, Chile, 2009, pp.71-82.

[34] B. Zhao, E. Jak, P.C. Hayes, Fundamental studies in ironmaking slags to lower operating temperatures and to recover titania from slag, *J. Iron Steel Res. Int.* 16 (2009) 1172-1178.

[35] Z. Wang, Q. Zhu, H. Sun, Phase Equilibria in the TiO_2-rich part of the TiO_2-CaO-SiO_2-10wt pct Al_2O_3-5 wt pct MgO system at 1773 K, *Metall. Mater. Trans. B* 50 (2019) 357-366. https://doi.org/10.1007/s11663-018-1441-2.

[36] Z. Wang, H. Sun, L. Zhang, Q. Zhu, Phase equilibria in the TiO_2 rich part of the TiO_2-CaO-SiO_2-10wt.% Al_2O_3 system at 1773 K and 1873 K, *J. Alloy. Compd*. 671 (2016) 137-143. https://doi.org/10.1016/j.jallcom.2016.02.044.

[37] J. Shi, M. Chen, X. Wan, P. Taskinen, A. Jokilaakso, Phase equilibrium study of the CaO-SiO_2-MgO-Al_2O_3-TiO_2 system at 1300 °C and 1400 °C in air, *JOM*, 72 (2020) 3204-3212. https://doi.org/10.1007/s11837-020-04136-1.

[38] J. Shi, M. Chen, I. Santoso, L. Sun, M. Jiang, P. Taskinen, A. Jokilaakso, 1250 °C liquidus for the CaO-MgO-SiO_2-Al_2O_3-TiO_2 system in air, *Ceram. Int.* 46 (2020) 1545-1550. https://doi.org/10.1016/j.ceramint.2019.09.122.

[39] J. Shi, L. Sun, J. Qiu, M. Jiang, Phase equilibrium investigation for CaO-SiO_2-5wt.% MgO-20wt.% Al_2O_3-TiO_2 system relevant to Ti-bearing slag system, *ISIJ Int.* (2018) ISIJINT-2017-2555. https://doi.org/10.2355/isijinternational.ISIJINT-2017-555.

[40] J. Shi, L. Sun, J. Qiu, B. Zhang, M. Jiang, Phase equilibria of CaO-SiO_2-5wt% MgO-10wt% Al_2O_3-TiO_2 system at 1300° C and 1400 °C relevant to Ti-bearing furnace slag*, J. Alloy. Compd.* 699 (2017) 193-199. https://doi.org/10.1016/j.jallcom.2016.12.328.

[41] J. Shi, L. Sun, J. Qiu, M. Jiang, Phase equilibria of CaO-SiO_2-5wt.% MgO-30 wt.% Al_2O_3-TiO_2 system at 1400 °C and 1450 °C relevant to high Al_2O_3 Ti-bearing blast furnace slag system*, J. Alloy. Compd.* 722 (2017) 25-32.https://doi.org/10.1016/j.jallcom.2017.06.058.

[42] J. Shi, L. Sun, B. Zhang, X. Liu, J. Qiu, Z. Wang, M. Jiang, Experimental Determination of the Phase Diagram of the CaO-SiO_2-5 pct MgO-10 pct Al_2O_3-TiO_2 System, *Metall. Mater. Trans. B* 47 (2016) 425-433. DOI: 10.1007/s11663-015-0527-3.

[43] J. Shi, L. Sun, J. Qiu, Z. Wang, B. Zhan, M. Jiang, Experimental determination of the liquidus in CaO-SiO_2-MgO-10%Al_2O_3-5%TiO_2 system, *J. Cent. South Univ*. 47 (2016) 3309-3314.

[44] X. Wan, J. Shi, L. Klemettinen, M. Chen, P. Taskinen, A. Jokilaakso, Equilibrium phase relations of CaO-SiO_2-TiO_2 system at 1400° C and oxygen partial pressure of 10^{-10} atm, *J. Alloy. Compd*. 847 (2020) 156472. https://doi.org/10.1016/j.jallcom.2020.156472.

[45] M. Chen, J. Shi, P. Taskinen, A. Jokilaakso, Phase equilibria of the CaO-SiO_2-TiO_2-Al_2O_3-MgO system in air at 1250-1400 °C, *Ceram. Int.* 46 (2020) 27702-27710. https://doi.org/10.1016/j.ceramint.2020.07.268.

[46] R. Davies, A. Dinsdale, J. Gisby, J. Robinson, M. Martin, MTDATA-thermodynamic and phase equilibrium software from the national physical laboratory, *Calphad*, 26 (2002) 229-271.

[47] C.W. Bale, P. Chartrand, S. Degterov, G. Eriksson, K. Hack, R.B. Mahfoud, J. Melançon, A. Pelton, S. Petersen, FactSage thermochemical software and databases, *Calphad*, 26 (2002) 189-228. https://doi.org/10.1016/S0364-5916(02)00035-4.

[48] N. Arora, P.L. Wenzel, S.L. McKinney-Freeman, S.J. Ross, P.G. Kim, S.S. Chou, M. Yoshimoto, M.C. Yoder, G.Q. Daley, Effect of developmental stage of HSC and recipient on transplant outcomes, *Dev. Cell* 29 (2014) 621-628. https://doi.org/10.1016/j.devcel.2014.04.013.

[49] M. Hillert, B. Sundman, X. Wang, An assessment of the $CaO-SiO_2$ system, *Metall. Trans. B* 21 (1990) 303-312.

[50] C. Soontrapa, Y. Chen, Optimization approach in variable-charge potential for metal/metal oxide systems, *Comput. Mater. Sci.* 46 (2009) 887-892. https://doi.org/10.1016/j.commatsci.2009.04.027.

[51] M. Chen, J. Shi, P. Taskinen, A. Jokilaakso, Experimental determination of the 1300 °C and 1400° C isotherms for $CaO-SiO_2-TiO_2$-10 wt% Al_2O_3 system in air, *Ceram. Int.* 46 (2020) 9183-9191. https://doi.org/10.1016/j.ceramint.2019.12.170.

[52] E. Jak, P.C. Hayes, H.G. Lee, Improved methodologies for the determination of high temperature phase equilibria, *Met. Mater*. 1 (1995) 1-8.

[53] L. Sun, J. Shi, Z. Yu, M. Jiang, Phase equilibria and liquidus surface of $CaO-SiO_2$-5 wt% $MgO-Al_2O_3-TiO_2$ slag system, *Ceram. Int.* 45 (2019) 481-487. https://doi.org/10.1016/j.ceramint.2018.09.193.

[54] L. Sun, J. Shi, C. Liu, M. Jiang, Phase equilibria studies for $CaO-SiO_2$-5wt.% $MgO-Al_2O_3-TiO_2$ system in high Al_2O_3 content area with w (CaO)/w (SiO_2) ratio of 1.50, *J. Alloy. Compd*. 810 (2019) 151949. https://doi.org/10.1016/j.jallcom.2019.151949.

[55] G. Bastin, J. Dijkstra, H. Heijligers, PROZA96: an improved matrix correction program for electron probe microanalysis, based on a double Gaussian φ (ρz) approach. *X Ray Spectrom.*, 27(1), (1998) 3-10. https://doi.org/10.1002/(SICI)1097-4539(199801/02)27:1<3::AID-XRS227>3.0.CO;2-L.

[56] D. Liu, J. Diao, G. Wang, B. Xie, Analysis of V and Cr with various valence states in $FeO-SiO_2-MnO-TiO_2-VO_x-MgO-CrO_x$ system by XPS method, *Metall. Res. Technol.* 116 (2019) 218. https://doi.org/10.1051/metal/2018075.

[57] I. Jung and M. Van Ende, Computational thermodynamic calculations: FactSage from CALPHAD thermodynamic database to virtual process simulation, *Metall. Mater. Trans.* B 51 (2020) 1851-1874. https://doi.org/10.1007/s11663-020-01908-7.

[58] C. Liu, J. Qiu, Z. Liu, D. Zhu, Y. Wang, M. Jiang, Adjacent relations of primary phase fields and invariant reactions of the system $CaO-SiO_2-Nb_2O_5-La_2O_3$, *J. Am. Ceram. Soc.* 104 (2020) 2398-2409. https://doi.org/10.1111/jace.17605.

[59] Z. Cao, X. Sun, Z. Qiu, Thermodynamic modeling software FactSage and its application, *J. Chin. Rare Metals*. 2 (2008) 216-219.

[60] J. Gisby, P. Taskinen, J. Pihlasalo, Z. Li, M. Tyrer, J. Pearce, K. Avarmaa, P. Björklund, H. Davies, M. Korpi, MTDATA and the prediction of phase equilibria in oxide systems: 30 years of industrial collaboration, *Metall. Mater. Trans. B* 48(1) (2017) 91-98. https://doi.org/10.1007/s11663-016-0811-x.

[61] R. DeVries, R. Roy, E. Osborn, Phase equilibria in the system $CaO\text{-}TiO_2\text{-}SiO_2$, *J. Am. Ceram*. Soc., 38 (5) (1955) 158-171. https://doi.org/10.1111/j.1151-2916.1955.tb14922.x.